UNIVERSITY OF CALIFORNIA

Los Angeles

Quantitative Characterization of Complex Coacervate Dispersions

A thesis submitted in partial satisfaction

of the requirements for the degree Master of Science

in Chemical Engineering

by

Vihar J. Trada

2024

ABSTRACT OF THE THESIS

Quantitative Characterization

of Complex Coacervate Dispersions

by

Vihar J. Trada

Master of Science in Chemical Engineering

University of California, Los Angeles, 2024

Professor Samanvaya Srivastava, Chair

Polyelectrolyte complex (PEC) coacervate dispersions are a versatile platform for the realization of aqueous colloidal encapsulants and bioreactors. The membraneless microdroplets comprising these dispersions form by liquid-liquid phase separation and introduce a distinct and unstable water-water interface with external aqueous environments, eventually leading to their coalescence and resulting in macro phase separation. This is a well-known phenomenon, that can be explained by conventional theories such as Voorn-Oberbeek (VO) model. Previously, we have shown that comb polyelectrolytes (cPEs) stabilize the coacervate microdroplets against coalescence, enabling the formulation of stable coacervate microemulsions. Stabilized PEC microdroplets possess

unique properties like higher salt resistance, an expanded two-phase region, stable compartmentalization over longer periods of time, and higher stability under diverse conditions like (temperature, pH, ionic strength). However, predictions of phase separation and phase composition are a major challenge upon addition of cPEs in PEC systems. In this study, we have rigorously studied one widely used PE system constructed of poly(diallyldimethylammonium chloride) (PDADMAC) as a polycation and poly(acrylic acid) (PAA) as a polyanion, while negatively charged MasterGlenium 7500 served as a cPE. This fundamental study aims to quantify phase composition using a series of thermogravimetric analysis. Along with rheology and high throughput turbidimetry measurements proving robustness of this stabilization strategy. Resorting to recent microfluidics advancements, a strategy to form monodisperse microdroplets is also discussed here. Overall, the results presented here will provide crucial information enabling a wide range of applications such as tailoring protocells and microreactors.

The thesis of Vihar J. Trada is approved.

Dante A. Simonetti

Thaiesha Andrea Wright

Panagiotis D. Christofides

Samanvaya Srivastava, Committee Chair

University of California, Los Angeles

2024

Table of Contents

1. Introduction

1.1 Background and applications

Mixing oppositely charged polyelectrolytes (PEs) often leads to the liquid-liquid phase separation forming polymer complexes via electrostatic interaction.[1,2] This process is entropically favorable due to the release of counterions from the charged macromolecules. Upon macroscopic phase separation, a distinct interface emerges between two phases: one enriched with neutralized polymer complexes and the other depleted of such complexes, as illustrated in Figures 1a and 2a. Numerous factors govern the complexation process, including charge density, polymer structure, and environmental parameters such as pH and ionic strength.[2,3] The resulting complexes, or coacervates, can exhibit a range of physical states—water-rich viscous formulations, soluble structures, precipitates, or hydrogels—with tunable properties suitable for varied applications.[4] However, majority of applications are restricted due to a major limitation which is macro-phase separation. The observation of this phenomenon dates as back as 1929 when the term “coacervate” derived from the Latin term “coacervatio” meaning “gathering into a pile” was coined by Bungenberg de Jong and Kruyt, thus, numerous studies use the term coacervation as complexation is a subset of coacervation. Voorn-Overbeek (VO) theory being the first in this list, many different models as well as improved VO models have been proposed to predict the extent of coacervation,[1] however, equal number of disagreements are also reported in experimental studies. Therefore, this study aims to demonstrate qualitative characterization of PEC dispersion solely relying on widely acknowledged experimental approaches like, high throughput turbidimetry to evaluate presence of coacervation and thermogravimetric analysis to quantify the composition of phase-separated PEC dispersion.[5,6]

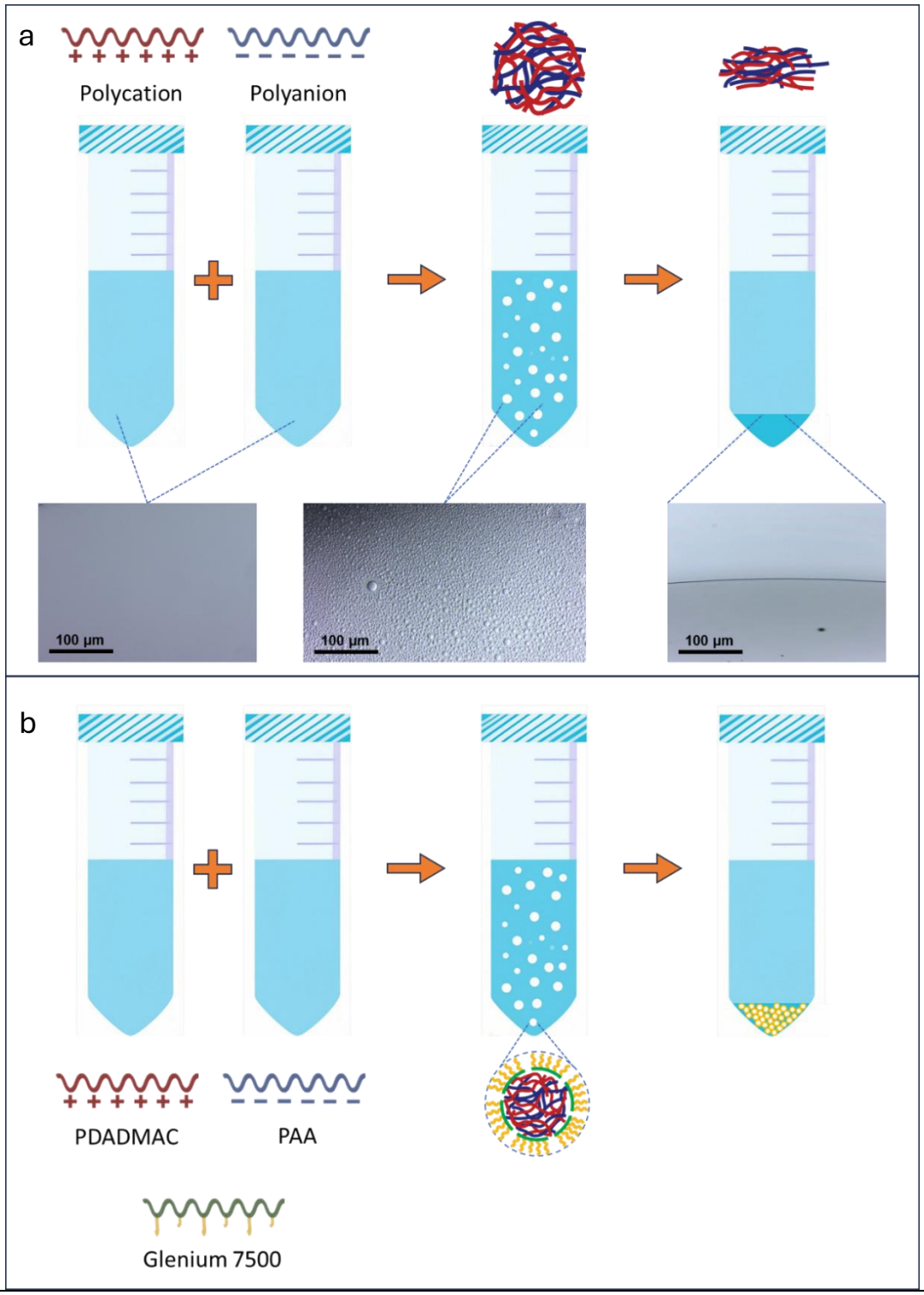

Figure 1: Simplified illustration of microdroplets formation by polyelectrolyte complexation. (a) shows entropy driven self-assembly of PEC that reaches phase equilibrium after a short period of time. (b) shows a schematic of PEC stabilization using comb-polyelectrolyte where droplets settle down due to gravity but do not phase separate.

A representation of a general binodal phase diagram in Figure 2a tells that any polyelectrolyte dispersion prepared at a given PE concentration (C) will phase separate into a supernatant phase containing a polymer concentration (C_s) and a denser coacervate phase with a higher polymer concentration (C_c). Phase separation can be terminated by the addition of salt at a critical concentration, known as the salt resistance (C_{SR}) of the dispersion. While the partitioning of polymer complexes between these phases is well-established, the partitioning of salt (including counterions released during coacervation) remains a matter of debate. The classical theory given by Voorn and Overbeek posits that at equilibrium, the total free energy per unit lattice site in k_BT units should be:

$$f_{total} = -\alpha \cdot [\sum_i \sigma_i \Phi_i]^{\frac{3}{2}} + \sum_i \frac{\Phi_i}{N_i} ln\Phi_i \quad \text{(i)}$$

Where, α is numerical factor composite of $2\sqrt{\pi}e^3 / 3\sqrt{v\epsilon^3(k_BT)^3}$ where, e is elementary charge, k_B is Boltzmann constant, T is temperature and ϵ is the permittivity of the solvent. The value of α should be approximately 3.655 for hydrophilic PEs.[2] N_i and σ refer to degree of polymerization and charge densities (z_i/N_i) of PEs. According to this model, the coacervate phase should contain a higher salt concentration compared to the supernatant phase. However, experimental evidence has frequently contradicted this model, particularly in studies involving synthetic polyelectrolytes with hydrophilic backbones and symmetric polymer lengths and charge densities.[2,6] Thus, a pair of similar PEs is used in this study which is Poly(diallydimethylammonium chloride) (PDADMAC) being polycation and charged poly(acrylic acid) (PAA) serving as polyanion. Coacervate droplets formed by these water-soluble polyelectrolytes feature unique properties upon phase separation due to the water-water interface that allows strong and effective partitioning or encapsulation of charge-bearing macromolecules such as proteins.[1,2,7–10] Also, many different

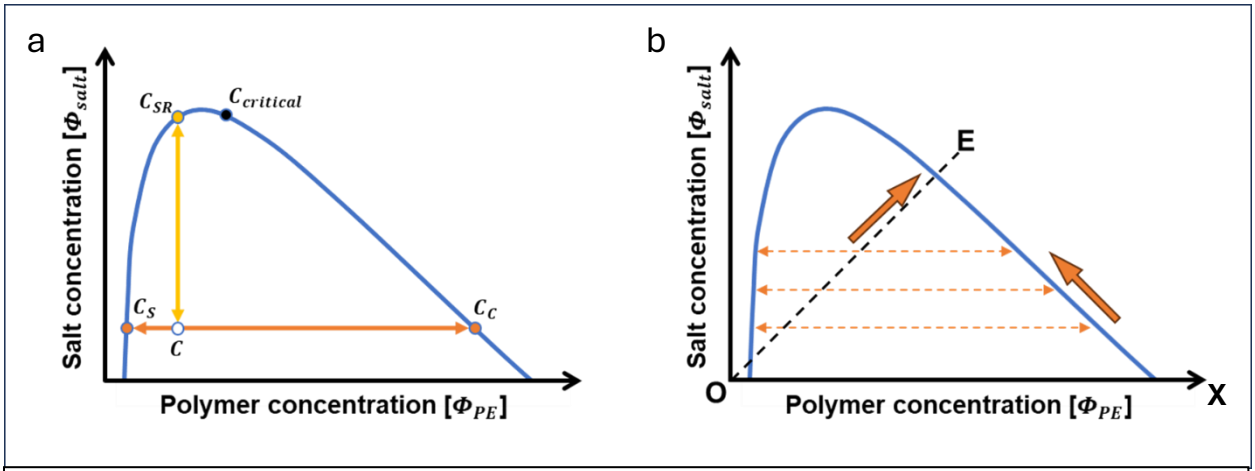

Figure 2: General schematic of the binodal phase diagram. The blue curve represents the boundary of 2 phase regime if only two parameters are varied: salt concentration (Φ_{salt}) and polymer complexes concentration (Φ_{PE}). (a) Any PEC dispersion prepared with composition corresponding to C, will phase separate into a supernatant phase containing polymer concentration at C_s and coacervate phase containing polymer concentration at C_c. The concentration of salt required to terminate this phase separation will be denoted as salt resistance C_{SR} of given dispersion. $C_{critical}$ is the critical point that usually takes place on right of the maxima of phase boundary. (b) indicates the variation in composition of both phases upon adding more salt. Line OE represents the equimolar balance between PEs and associated counter ions.

coacervate droplets show no information exchange when different droplets carrying different molecules come into close contact with each other.[7,10] Dense core of these complex coacervate droplets can facilitate multiple different enzymes improving the enzymatic activity and reaction rates when cascade of reaction is targeted making them a promising candidate for colloidal micro reactors.[3,9,11–14] Considering all these factors, this pair of PEs presents a strong case for their application as micro-reactors. Thermogravimetry analysis on supernatant and coacervate phases independently will quantify the actual composition of both phases precisely, and varying the total PE concentration (Φ_{PE}) can reveal the true (experimental) two-phase regime boundary which can be crucial information for tailoring size of microdroplets and their physical properties. In practical settings, adding more PEs will follow the O→E path shown in Figure 2b, rather than O→X as

counterions released from each PE during complexation, Na^+ and Cl^-, will act as salt. This will be applicable throughout this study whenever, increase of Φ_{PE} is mentioned.

While complex coacervation is a result of thermodynamic equilibrium, it also restricts majority of applications. Macro-phase separation of dispersions does not favor most of their applications as the specific surface area of the coacervate phase goes down by many folds upon droplet coalescence. Numerous studies have suggested solutions to tackle this issue, such as introducing hydrophobic phases composed of lipid, but there are major limitations in implementation as the layer stabilizing droplets will also increase the barrier for mobility of charged hydrophilic molecules while diffusing in and out of each stable microdroplet. Previously, we have shown a way to provide robust stabilization to PEC microdroplets while retaining core advantages, utilizing comb polyelectrolyte (cPEs). Addition of cPEs will prevent the coalescence of droplets and restrict macro-phase separation, reducing the depletion in the specific surface area water-water interface. Due to electrostatic interactions, charged backbones of cPE settle at this interface forming a uniform corona around each droplet as shown in Figure 1b. This simple yet effective assembly provides steric hinderance against coalescence, thus, the shape of droplets stays intact even in a closely packed environment.[15] Previously, we presented a high throughput screening method based on turbidimetry that can provide insight into expansion of binodal phase diagram, improved salt resistance and stability of these droplets over a long period of time up to 15 days. In this study, we demonstrate remastered protocol for the high throughput turbidimetry screening that will ensure reproducibility of the data with low deviations. Compared to our previous investigation, the composition point density in this set of experiments was increased by a fold, providing highly accurate phase boundary upon addition of MasterGlenium® 7500 (cPE used in these studies). Moreover, shear rheometry measurements done on stabilized dispersion

confirmed robustness of this stabilization strategy even under dynamic flow. Moreover, a microfluidic method was also explored to control the size distribution of PEC microdroplets in dispersion state. Utilizing the results of this study, the formation of monodisperse microdroplets is also possible that is discussed towards the end. Overall, this fundamental study aims to lower the barrier restricting advanced applications of PEC microdroplets.

2. Materials and Methods

2.1 Materials and Preparation of Stock Solution

Poly(acrylic acid sodium salt) (PAA, M_w = 5100 g mol^{-1} with chain length (n) of 53 and density of 0.55 g ml^{-1} at 25 °C) and sodium chloride (NaCl) were obtained from Milipore sigma. An aqueous solution of Poly(diallydimethylammonium chloride) (PDADMAC, M_w = 8500 g mol^{-1}, and n = 54 28% w/v in water) was sourced from Polysciences Inc. Comb polyelectrolyte used for this investigation was polymethacrylic acid-comb-polyethylene glycol ($PmAA_{45}$-comb-PEG_{68}, pH = 6, polydispersity index of 1.85 and density = 1.049 g ml^{-1}) having 12 PEG side chains for each polymethacrylic acid chain which was obtained from Master Builders Construction Chemicals.

Stock solutions of PAA and PDADMAC were prepared using mili-Q water at 2 different concentrations, 2 and 28% w/w, and vortex mixed for 1 minute, followed by a debubbling step through bath sonication for 10 minutes to get clear solutions. 23.38% w/w stock solution of sodium chloride was prepared using mili-Q water and vortex mixed for 1 minute to obtain clear homogeneous solution. The stock solution of comb polyelectrolyte given by manufacturer was identified to be at 9.1776% w/v and it was used without diluting it further.

2.2 Preparation of Coacervate Dispersions

Coacervate dispersions were prepared manually in 50 mL centrifuge tubes. Charge-balanced volumes of polyelectrolyte stock solutions were calculated to create a total volume of 40 mL per dispersion. To achieve the target volume, balancing amount of Milli-Q water was added

first, followed by the polycation, poly(diallyldimethylammonium chloride) (PDADMAC) stock solution, and then the polyanion, poly(acrylic acid) (PAA) stock solution. Each component addition was followed by vortex mixing for 20 seconds, with a final mixing of 1 minute after all components had been combined to ensure homogeneity.

Once mixed, 10 mL of each homogenous dispersion, representing uniform complex concentrations, was set aside for further analysis. The remaining dispersions were subjected to centrifugation at 5000 rpm for 20 minutes to initiate phase separation. For highly concentrated samples, no clear phase boundary was observed between the supernatant and coacervate phases immediately after centrifugation. Therefore, all the samples were allowed to rest on the benchtop for an additional 24 hours to enable gravity-driven settling, resulting in a distinct and well-defined interface between the two phases.

2.3 Thermogravimetric Analysis

Thermogravimetric analysis (TGA) was performed on 30 μg of freshly extracted (avoiding evaporation of solvent) coacervate samples isolated from each centrifuged dispersion to evaluate composition of each dispersion upon varying the concentration of polyelectrolytes.

The TGA analysis was carried out using a PerkinElmer TGA 8000 instrument, with samples loaded into ceramic pans. Mass loss data were recorded at a rate of 1 Hz to ensure precise monitoring of thermal events. The thermal program involved a multi-step temperature profile designed to evaluate water content and other volatiles:

1. The coacervate samples were initially heated from 35.00 °C to 110.00 °C at a controlled rate of 50.00 °C/min to monitor the evaporation of solvent and/or moisture.
2. At 110.00 °C, an isothermal hold was maintained for 30 minutes, providing sufficient time to drive off remaining solvent and ensure stability at elevated temperature.
3. Thereafter, the samples were heated further to 650 °C from 110.00 °C at a rate of 100.00 °C/min, allowing complete degradation of polymer complexes.
4. At 650 °C, again an isothermal hold was maintained for 2 minutes (till mass loss stability was reported) and remaining contents in the pan would be only the mass of counter-ions.
5. Lastly, samples were cooled down to 35 °C from 650 °C at a controlled rate of 150 °C /min for assessment of potential residual effects upon returning to room temperature (like thermal drifts affecting transducer measurements).

However, the same protocol could not be followed for supernatant samples as majority of them contained high amounts of solvent (water) and above 110 °C, the samples would start boiling so, it would create splash and spill generating excessive noise. Therefore, another multi-step temperature profile was made which follows this sequence:

1. The supernatant samples were initially heated from 35 °C to 80 °C at a controlled temperature rate of 50 °C/min to monitor a partial evaporation of solvent.
2. At 80 °C, an isothermal hold was maintained for 5 minutes providing sufficient time to reduce the mass of sample to less than half.
3. After that, the samples were heated to 110 °C from 80 °C at a constant rate of 15 °C/min in order to remove solvent completely.

4. Again, the samples were given sufficient time (5 minutes) to establish thermal equilibrium ensuring no solvent/moisture was remaining within samples.
5. Lastly, each sample was heated to 650 °C at rate of 100 °C/min and complete degradation of polyelectrolytes was observed within 2 minutes.
6. Remaining measurements after this step provided information of counter ion concentration in supernatant samples and remaining mass was cooled down to 35 °C at rate of 100 °C/min assessing any potential residual effects upon returning to room temperature.

These heating protocols allowed for a comprehensive evaluation of each coacervate sample's thermal stability and provided insights into the mass loss associated with specific temperature changes.

2.4 Rheology Measurements

The steady shear viscosity (η), of coacervates and supernatant extracted from each dispersion as well as homogenous dispersions, was characterized using an Anton Paar MCR 302 Rheometer equipped with cone-and-plate geometry. Two sizes were utilized: a 10 mm diameter cone with a 1° cone angle for highly viscous samples (coacervate samples), and a larger 50 mm diameter cone with the same angle for water like samples (supernatant samples and stabilized dispersions). This rheometer, with a torque range of 2 nN·m to 200 mN·m, provided sensitive and accurate measurements under low-torque conditions.

Rheological measurements were conducted by imposing shear rates ($\dot{\gamma}$) between 10^{-1} and 10^{3} s^{-1}. The corresponding shear stress (τ_{12}) was also measured under these imposed shear rates, allowing for a detailed assessment of the coacervate samples' flow properties and response to

applied shear. All measurements were performed at a constant temperature of 25 °C, maintained by a Peltier element, to ensure thermal stability and reproducibility.

2.5 High Throughput Preparation of Coacervate Dispersions

High-throughput preparation of coacervate dispersions was conducted using the Fluent Automated Workstation by Tecan, a platform capable of precision liquid handling and scalable sample preparation. Fisher brand nunc transparent flat-bottom 96-well plates were used to prepare samples in, allowing real-time visual inspection of the solutions. Each well contained 200 µL of PEC dispersion, prepared by sequentially mixing specific volumes of polycation, polyanion, comb-polyelectrolyte (cPE), and sodium chloride (NaCl) stock solutions.

The preparation sequence within each well was rigorously controlled to optimize coacervate formation and avoid premature phase separation by adding the polyanion in the end, controlling the initiation of droplet formation constantly throughout 96 wells. The order of addition followed a defined protocol: first, Milli-Q water was added to each well to fix the final volume, followed by polycation, comb-polyelectrolyte, salt, and finally, the polyanion. Each polyelectrolyte component was dispensed by carefully submerging the pipette tips into the liquid within the well to prevent bubble formation and ensure uniform mixing while avoiding time dependent errors. To further optimize liquid handling, pipetting speed and liquid level detection settings were carefully adjusted. These modifications were essential to ensure accurate volume transfer, minimal liquid splashing, and efficient drop-by-drop addition without loss of material.

Following the addition of comb-polyelectrolyte and polyanion components, mixing was achieved by aspirating and dispensing a 100 µL volume three times, using the automated system's

liquid-handling arm. This repetitive mixing method ensured thorough mixing of each component, promoting homogeneity within each well and facilitating consistent coacervate formation across the entire 96-well plate. This procedure allowed for rapid, reproducible preparation of coacervate dispersions, providing an efficient workflow for high-throughput studies on coacervate phase behavior and composition.

2.6 Absorbance Measurements

Absorbance measurements, including single-wavelength and kinetic multi-wavelength scans, were performed using the Tecan Spark multimode microplate reader to evaluate the optical properties of coacervate dispersions. For single-wavelength measurements, absorbance at 400 nm and at 25 °C was monitored to assess the uniformity and optical density of the dispersions within each well. These measurements were conducted across 9 distinct spots per well and averaged out, providing a spatially resolved absorbance profile and enabling detection of micro droplets.

To ensure sample homogeneity prior to each measurement, the microplate was subjected to a 5-second orbital shaking step at a 2 mm amplitude, effectively redistributing any suspended particulates. This brief agitation minimized concentration gradients and sedimentation effects that could impact absorbance accuracy. The Tecan Spark microplate reader's scanning capability ensured reliable, high-throughput absorbance data collection, which was critical for detailed comparative analysis across high throughput analysis.

2.7 Optical Microscopy

Optical microscopy was employed to visualize and characterize the formation of coacervate droplets in PDADMAC-PAA dispersions, both in the presence and absence of stabilizing agents. Imaging was conducted on an inverted microscope (Motic AE31 Elite Trinocular Inverted Phase Contrast Microscope) with three plan Achromat objectives: 10x, 20x and 40x objectives, which provided high-resolution observation of droplet morphology and stability under varied conditions.

For static imaging, droplets were prepared on glass slides to observe their shape, size, and distribution in detail, capturing insights into the coacervate's phase behavior and interactions with stabilizers. This setup enabled direct comparison of droplet characteristics with and without the stabilizing agents, highlighting their influence on coacervate microdroplets structure.

In addition to static imaging, the Motic AE31 Elite was also utilized for live visualization of microfluidic droplet formation of PDADMAC-PAA. This allowed real-time observation of droplet size, growth, and stabilization dynamics within a controlled flow environment.

2.8 Microfluidics

A pre-made microfluidic flow focusing droplet generator devices were purchased from Darwin Microfluidics (Fluidic 947 and Fluidic 440). It was employed to facilitate controlled flow conditions for the experimental investigations. The microfluidic chip was fabricated using polycarbonate (PC) that provided natural hydrophobic channels, with a feature height of 175 μm and a channel width varying from 10 to 80 μm.

Fluid delivery was managed using two syringe pumps (NewEra Pump systems SyringeONE NE-1000), capable of delivering flow rates ranging from 0.73 µL/hr to 2100 ml/hr. 1 ml syringes were connected to the inlet ports of the microfluidic chip using flexible, chemically resistant 1/16" ID Tygon tubing to ensure compatibility with the experimental reagents. To avoid bubble formation and ensure consistent flow, all reagents were degassed in bath sonication prior to loading in the syringes.

Real-time monitoring of flow behavior and device performance was achieved using an inverted optical microscope (Motic AE31 Elite Trinocular Inverted Phase Contrast Microscope) equipped with 4 different objectives (4x, 10x, 20x, and 40x) and a high-resolution 4K camera (Moticam A16). Images and videos were captured at 30 frames per second for post-analysis. The microfluidic setup was rigorously cleaned with high concentration salt solution (4M NaCl) after each experiment to prevent cross-contamination, involving sequential washes with DI water, followed by air drying. Device integrity was verified through optical inspection in the case of reuse.

3. Results and Discussion

3.1 Composition of PEC Dispersions

Quantitative and precise knowledge of phase compositions is highly beneficial for understanding, 1.) the physical properties they attribute and 2.) stabilization the PEC droplets through cPEs. To simplify the composition study, no stabilizers were added as hypothesis of cPE-driven stabilization states that the addition of cPEs does not affect the composition of droplets in any way. Macro-phase separation in unstable dispersions was accelerated in centrifuge at 4696 × *g*, allowing independent phase analysis of the complex coacervate and supernatant phases, as shown in Figures 3 and 4. The dispersions were prepared by mixing aqueous stock solutions of the polycation and polyanion, resulting in samples containing inherent salt content. This salt originated from counterions released during complex coacervation, that also influences the composition of each phase.

As illustrated in Figure 2b, the composition of the polyelectrolyte dispersion followed the O →E path, rather than the O →X path, when the initial polyelectrolyte concentration ($\Phi_{PE,0}$) increased. Dispersions at higher $\Phi_{PE,0}$ but still falling within the binodal phase boundary, contained more counterions as a byproduct of coacervation. This increased the density of free salt ions in the dispersion, which would interfere with the electrostatic interactions between polyanion and polycation chains via charge screening and as a result, the water content in the complex phase increased. Conversely, at lower $\Phi_{PE,0}$, fewer counterions should be present in each phase, reducing water content in the complex phase—a phenomenon widely recognized as the self-suppression effect.

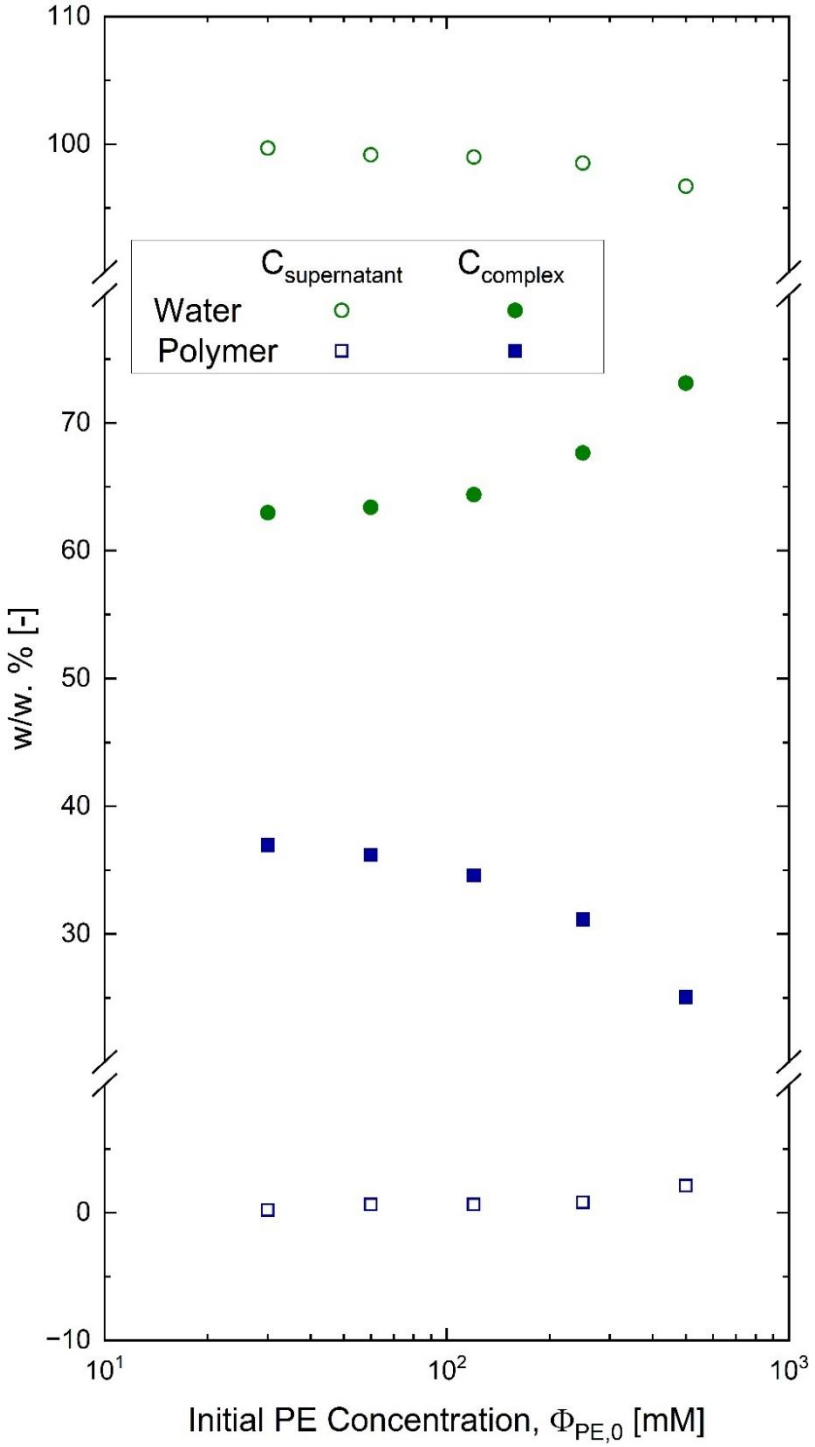

Figure 3: Thermogravimetric analysis of coacervate and supernatant samples extracted from phase separated dispersions containing PE concentrations at 30, 60, 120, 250, and 500 mM

As per Figure 3, when $\Phi_{PE,0}$ increased from 30 to 500 mM, the water content in the coacervate phase rose from 63% to 73% by weight, while polymer content declined from 37% to 25%. These trends indicate a diminishing of the self-suppression effect with increase in $\Phi_{PE,0}$, mostly due to the charge screening effects.

Tie-lines connecting the compositions of the supernatant and complex phases, shown in Figure 4a, exhibited positive slopes. This suggests preferential partitioning of salt into the complex phase which is consistent with V-O theory, though the observed salt partitioning was 1.5-2.5x higher than predicted, except for the lowest concentrated sample (30 mM) as shown in Figure 4b. The predictions of $P_{C/S}$ were made using the following equation derived from V-O model:

$$\ln\left(\frac{\Phi_{PE,C}}{\Phi_{PE,S}}\right) \approx \sigma N \cdot \ln\left(\frac{\Phi_{Salt,C}}{\Phi_{Salt,S}}\right) \quad \text{(ii)}$$

Where, $\Phi_{PE,C}$ and $\Phi_{Salt,C}$ are polymer and salt concentrations in complex phase, and $\Phi_{PE,S}$ and $\Phi_{Salt,S}$ are polymer and salt concentrations in supernatant. Again, σ is charged density of nearly symmetric PEs and N is degree of polymerization. Using experimentally determined polymer concentrations in both phases, theoretical predictions for the salt concentration ratio were calculated. The results showed that at increasing salt concentrations (Φ_{Salt}) in the dispersions, the partition coefficient ($P_{C/S}$) gradually lowers to ~1, signifying nearly equal salt partitioning but favoring complex phase by a small margin. This trend, in turn, reduced the gradient of Φ_{PE} across the two phases mainly due to charge screening and as a result, contrast in composition of both phases eventually disappears upon increasing $\Phi_{PE,0}$ further. If not due to counterions concentration, then at sufficiently high added salt levels, the dispersions no longer exhibited phase separation, as predicted by the model. This has further discussed in high-throughput results.

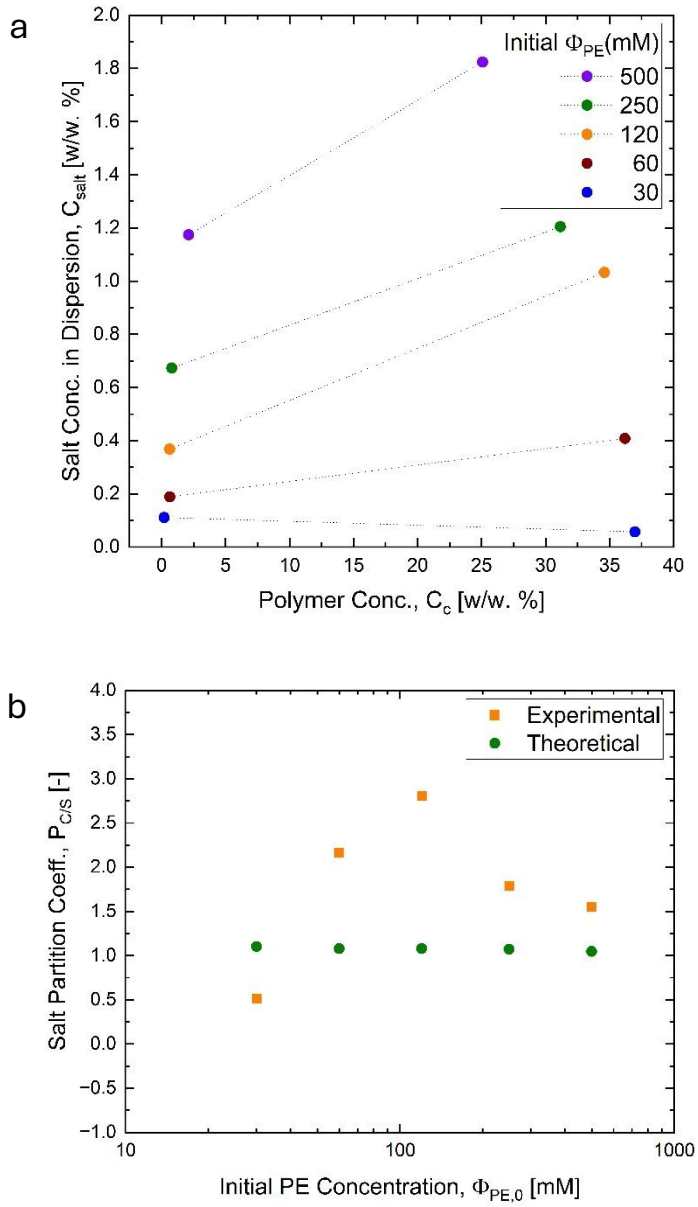

Figure 4: (a) Complete polyelectrolyte complexation phase diagram for dispersions comprising $PDADMAC_{53}$-PAA_{54}. (b) Salt partition coefficients ($P_{C/S}$) for $PDADMAC_{53}$-PAA_{54} as a function of Φ_{PE}. Experimental $P_{C/S}$ initially increases upto certaining critical Φ_{PE} and then, declines towards an equilibrium ~1. Theoretical $P_{C/S}$ values are predicted by V-O theory

3.2 Flow Behavior of PEC Dispersions

Rheological measurements can provide insights into the flow behavior of PEC dispersions that can be crucial for processing them, for example, in microfluidics.[16,17] Viscosity as a function of shear rate ($\dot{\gamma}$) was measured for both the supernatant and coacervate phases over a range from 0.1 s^{-1} to 1000 s^{-1} using cone and plate geometry. These measurements reveal distinct rheological characteristics arising from differences in composition and structure between the two phases. The viscosity measurements, shown in Figure 5, demonstrate a stark difference between the two phases. Supernatant aliquots from all the dispersion exhibit nearly water-like behavior, characterized by a constant viscosity (η) across the entire shear rate range. The low viscosity of the supernatant phase reflects its composition, which is predominantly water with minimal polyelectrolyte and salt content. On the other hand, complex phase samples displayed pronounced shear-thinning behavior in the first half of the shear sweep, where viscosity decreases significantly with increasing shear rate. This non-Newtonian behavior can be indicative of a dense polymer network made of complexes within the coacervate phase.[6]

The shear-thinning behavior of the coacervate phase samples is consistent with the disruption of polyelectrolyte chain entanglements and relaxation of electrostatic interactions under applied shear. At low shear rates ($\dot{\gamma}$), they exhibit high viscosity due to the dominance of intermolecular electrostatic interactions and entanglements. As the shear rate increases, these interactions are progressively overcome, leading to a reduction in viscosity. In the second half, above a certain shear rate (~10 s^{-1}), the internal structure/packing of the complexes would be perturbed to the maximum extent possible in shear flow, causing the viscosity to become relatively constant (Newtonian fluid-like behavior) and no longer decrease with further increases in shear rate.

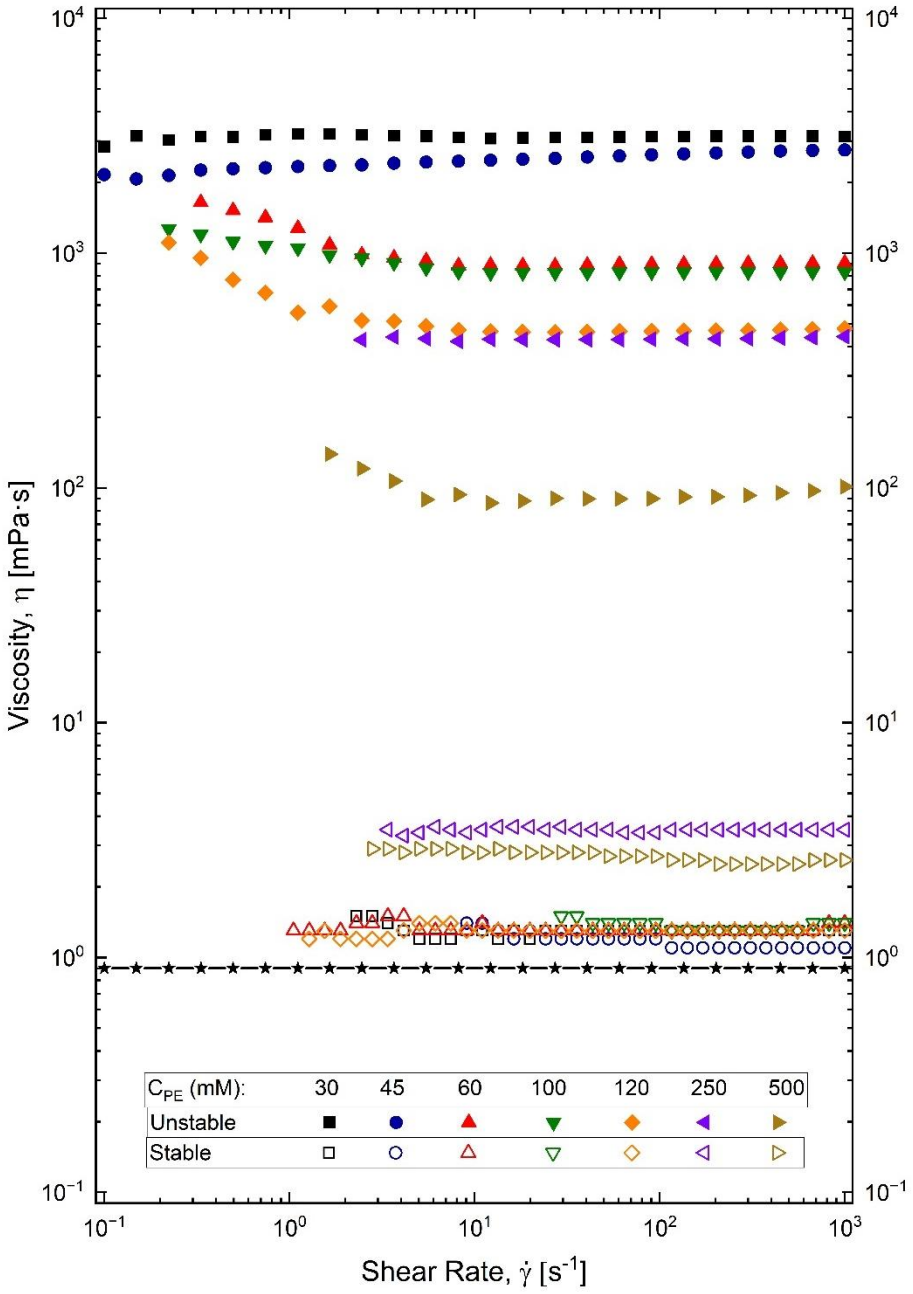

Figure 5: For unstable dispersions, complex coacervate and supernatant phases were analyzed separately. For a comparison, average supernatant phase viscosity for all the dispersion is referred by black stars connected by a solid black line. Every stable dispersion contained 8 mM of Glenium 7500. All 7 complex coacervate samples were measured using 10 mm cone and plate. Rest of all samples were measured using 50 mm cone and plate

In Figure 5, a clear trend emerges in the flow behavior of the coacervate phase at higher shear rates (>10 s^{-1}). As the initial polyelectrolyte concentration $\Phi_{PE,0}$ increases from 30 mM to 500 mM, the corresponding viscosity decreases significantly, from 3121.5 mPa·s to 89.7 mPa·s. This trend is further quantified in Figure 6, which illustrates the relationship using an allometric model. The fit suggests that the coacervate phase swells in response to the presence of additional counterions in the system, enhancing the spatial flexibility of the complexes under shear. This structural adaptation is reflected in the flow behavior, with an average viscosity reduction of 1.21 mPa·s per millimolar increment in $\Phi_{PE,0}$.

Interestingly, shear rheometry on unstable dispersions revealed that the composition of $PDADMAC_{53}$-PAA_{54} systems can be inferred from their rheological properties. However, this relationship does not translate to stable dispersions, where the complex phase exists as micro-sized droplets dispersed throughout the medium, rather than forming a separate macro-phase at the

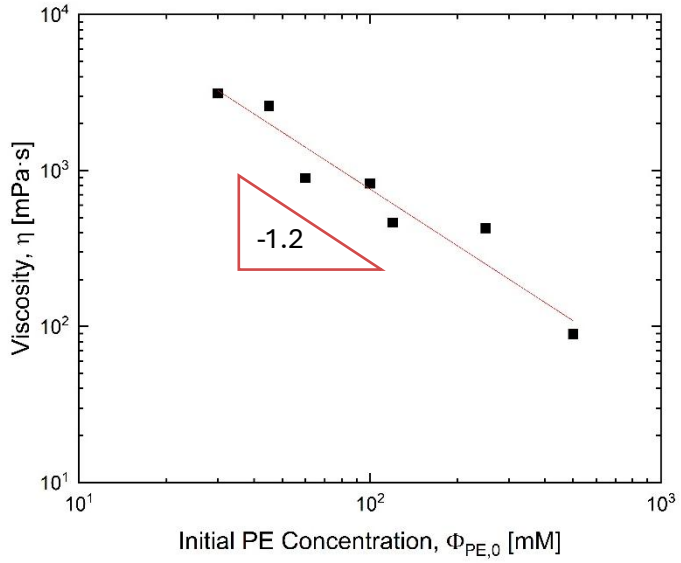

Figure 6: Viscosity of complex phase as a function of $\Phi_{PE,0}$ in unstable dispersions. Red line indicates allometric fit with $R^2 = 0.92$.

bottom, as observed in unstable dispersions. In stable dispersions, the comb-polyelectrolyte (cPE)-driven stabilization of PEC microdroplets imparts significant resistance to shear stress across the applied range (0.2 mPa–3.5 Pa).

Open symbols in Figure 5 represent the viscosity of stable, nearly homogeneous dispersions containing PEC microdroplets stabilized by cPE. In this study, all stable dispersions contained 8 mM of constant cPE (Glenium) concentration, while $\Phi_{PE,0}$ was varied from 30 mM to 500 mM. Regardless of the variation in $\Phi_{PE,0}$, these dispersions exhibited Newtonian fluid-like flow behavior throughout the applied shear rate range. While samples with higher $\Phi_{PE,0}$ showed increased viscosity, this is consistent with the expectation that since, the cPE concentration remained constant, the increased $\Phi_{PE,0}$ likely led to larger droplet sizes, as discussed further in the next section.

These findings underscore the robustness of cPE-driven stabilization, which maintains dispersion stability and shear resistance even under extreme flow conditions. The ability of this approach to preserve microdroplet structural integrity highlights its potential for applications requiring flow stability in complex coacervate systems.

3.3 Comb Polyelectrolyte-Driven Stabilization of PEC Microdroplets

MasterGlenium 7500, cPE used in this study has two major features: charged backbone and neutral hydrophilic side chains. While a negatively charged backbone attracts PEC microdroplets, neutral hydrophilic PEO side chains favor water-rich supernatant and as a result, the cPE backbone takes place at the liquid-liquid interface facing side chains away from droplets.[5,15] This unique structure "corona-like" geometry of cPE around each droplet provides steric hinderance against coalescence. Even in a crowded environment (once droplets settle down), or in high ionic strength conditions, where salt screens electrostatic interactions between oppositely charged PEs, a single layer of cPE can prevent merger of two droplets.

The size of stabilized PEC microdroplets is governed by two primary factors: the coacervate phase volume and the concentration of the comb polyelectrolyte (cPE).[5] These factors collectively determine the balance between droplet formation and stabilization. We hypothesize that microdroplet sizes are controlled by the ratio of the coacervate phase volume, dictated by $\Phi_{PE,0}$ and Φ_{Salt}, to the interfacial area that can be stabilized, which depends on the concentration of comb polyelectrolyte (Φ_{cPE}). As Φ_{cPE} increases, the total number of cPE chains can stabilize a larger interfacial area, while the coacervate phase volume remains constant. This results in the formation of more, smaller microdroplets and a corresponding decrease in the initial average microdroplet diameter (d_0). In contrast, increasing Φ_{Salt} leads to an expansion of the coacervate phase volume due to higher water content in the phase. Since the stabilizable interfacial area remains relatively constant at fixed Φ_{cPE}, the microdroplets grow in size, leading to larger d_0. This phenomenon is also reflected in rheological measurements in Figure 5.

In the past, with DLS experiments, we have demonstrated that a plateau in d_0 would be observed with increasing Φ_{cPE} at constant $\Phi_{PE,0}$, suggesting that microdroplet size does not continually decrease with excess cPE addition.[5,15] This behavior may result from the formation of secondary structures, such as cPE bilayers or vesicular assemblies, which reduce the efficiency of further interfacial stabilization. The same studies have extended the understanding of microdroplet stabilization mechanisms and established the versatility of cPEs across diverse polymer chemistries, salt concentrations, and mixing protocols. Previous high throughput study using $PDADMAC_{53}$-PAA_{54} proved that adding cPEs consistently stabilized PEC microdroplets in systems with varying polyelectrolyte (PE) compositions, salt types, and concentrations. Without cPEs, dispersions underwent rapid coalescence and macrophase separation, with settling evident within hours, particularly in the presence of salt. In contrast, the introduction of cPEs maintained droplet stability over extended periods, with no coalescence observed for up to 48 hours under typical conditions and no macrophase separation over months.[5]

Figure 7 shows reproduced data for the high throughput experiments reported in these investigations but using a modified experimental protocol. These experiments aimed to obtain binodal phase diagram of $PDADMAC_{53}$-PAA_{54} upon addition of comb polyelectrolytes. The formation of phase diagrams relied on turbidimetric measurements done on the dispersions right after preparing them. Using a Tecan Spark plate reader, absorbance (at 400 nm) of each stable PEC dispersion prepared with different compositions was measured which was converted to turbidity using following equation:

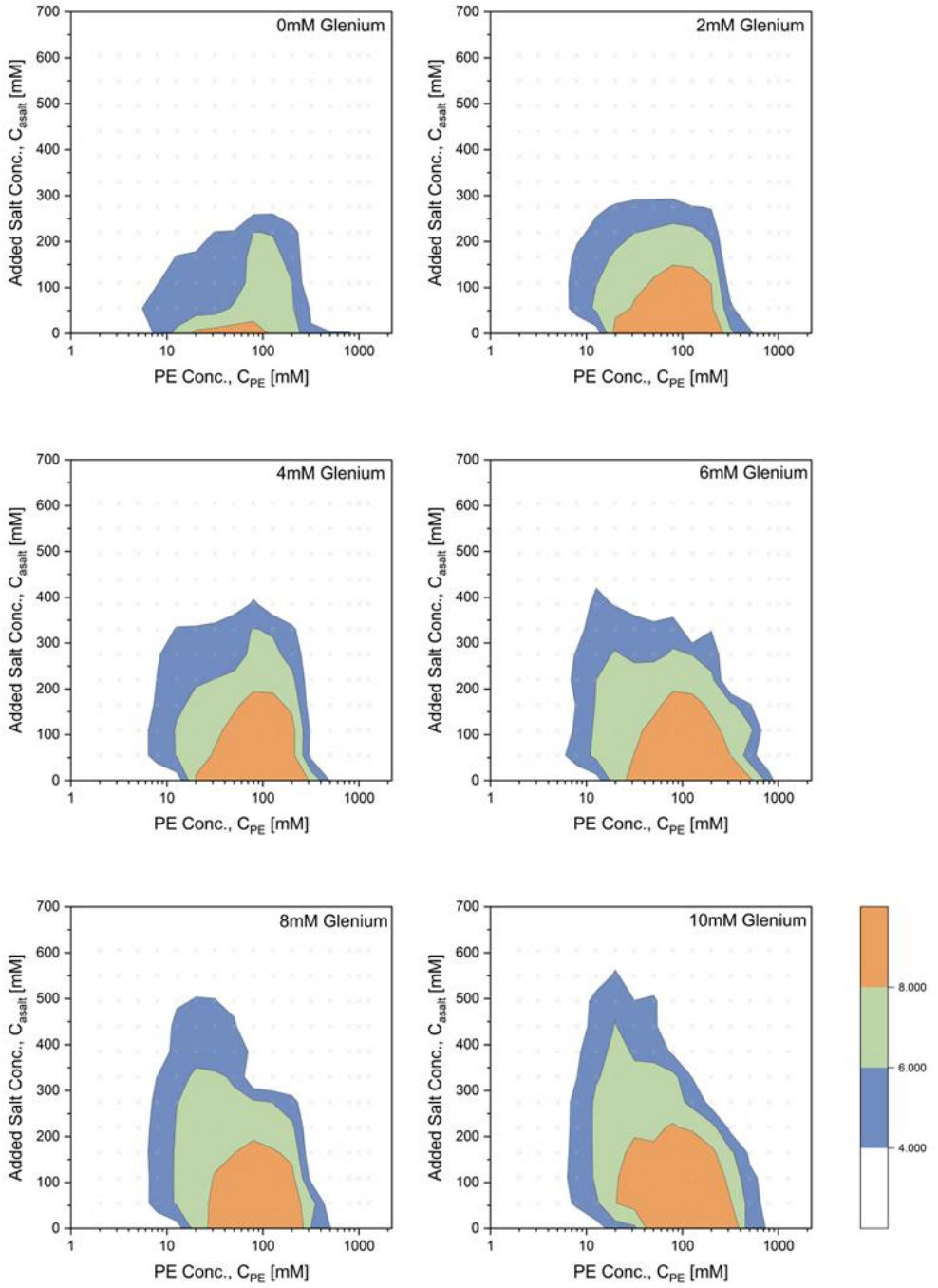

Figure 7: Addition of comb polyelectrolytes stabilize complex coacervate dispersions up to higher salt concentrations. All the contours show turbidity of dispersions as mixed. The cross symbols in the background indicate the composition of each dispersion that was measured.

$$T = ln\,(10) \cdot \frac{A}{l} \quad \text{(iii)}$$

Where, A and T refers to absorbance and turbidity, and l is the path length of the absorbance measurements.

When the mixing order was kept constant for all the repeated experiments, extreme deviations were observed in between multiple attempts suggesting a lot of room for improvement. Therefore, various parameters of high-throughput protocol were optimized including liquid class, conductivity, liquid level detection in stock solution vials, aspirating and dispensing speed as well as volumes. Apart from optimizing all these parameters, 2 more important factors were introduced in updated protocol which are: 1) time delays between preparing the samples and measuring the absorbance of the samples were suppressed to < 1 minute, 2) at constant C_{cPE}, number of compositions (varying Φ_{Salt} and Φ_{PE}) being tested to generate one contour, were increased from 88 to 192. Listed changes and optimizations, showed drastic improvement. While previous study reported C_{SR} of 100 mM NaCl for unstable dispersions, improved protocol consistently suggested 262 mM NaCl for the same system. The variation consistently showed an increment of 50 mM in salt resistance values reported in the previous study.

3.4 Microfluidic Formation of Monodisperse PEC Droplets

The development of techniques for producing monodisperse polyelectrolyte complex (PEC) microdroplets is critical for advancing applications in drug delivery[17–19], biocatalysis, and tissue engineering.[20,21] Monodispersity ensures uniformity in size and properties, which is essential for achieving consistent performance in these applications. Microfluidic methods offer unparalleled control over droplet formation, enabling precise tuning of droplet size, morphology, and composition. But unlike simple immiscible fluid droplet systems like oil-in-water or water-in-oil that rely on surface tension and or Plateau-Rayleigh instabilities for breaking up a continuous stream into droplets, the breakup of water-in-water kind of droplets in case of coacervates requires continuous shearing of coacervate filament until it breaks apart into droplets. Many different studies have shown methods to prepare monodisperse PEC droplets leveraging microfluidic techniques like increasing channel length, resulting in higher hydrostatic pressure being applied on droplets increasing the shear at low capillary number conditions.[7] However, this approach requires precise control over flow rate using pressure-driven pump removing even micro-oscillations in the inlet, and specific channel geometry (unusually longer length) that may not be a financially viable option. In addition, traditional stabilizers like surfactants used in immiscible systems may not work on PEC droplets. We demonstrate that the PDADMAC-PAA system is processable in a microfluidic environment and stabilization achieved with Glenium can also be translated into microfluidics, utilizing a simple cost-effective apparatus. We demonstrate a robust and reproducible approach to PEC microdroplet formation for this selected system, setting the stage for its broader application in precision-engineered systems.

Figure 8: Schematic of the microfluidic flow-focusing channel structure used to dispense bulk homogeneous coacervates into relative supernatant. All the channels at the junction are 30 µm and the outlet is expanding to 80 µm gradually. Homogeneous bulk coacervate phase enters the junction from left and is pinched and focused by a much faster sheath flow of supernatant stream entering the junction from the channels at the top and bottom.

Polycarbonate chips with hydrophobic inner surface were sourced from a commercial vendor and flow streams were regulated using 2 independent syringe pumps with 1 ml syringes. Figure 8 shows a flow-focusing microfluidic channel structure on dispersing a continuous aqueous coacervate stream into membrane-free coacervate droplets in a continuous PE lean supernatant stream. Hydrostatic pressure can be regulated by reducing the channel width as well instead of shearing the coacervate stream for a longer length scale, which is shown in Figure 8. For all microfluidic experiments, the coacervate stream was extracted from a 100mM unstable phase-separated solution. Flowrates of both streams in the device were also kept constant at 12 µL/hr for the coacervate stream and 240 µL/hr, fixing the supernatant to coacervate flow ratio at 20x, within a suitable range for any droplet generation.[17] While droplet generation was observed right after the junction, the droplets separated out of the supernatant due to a high number of coalescences.

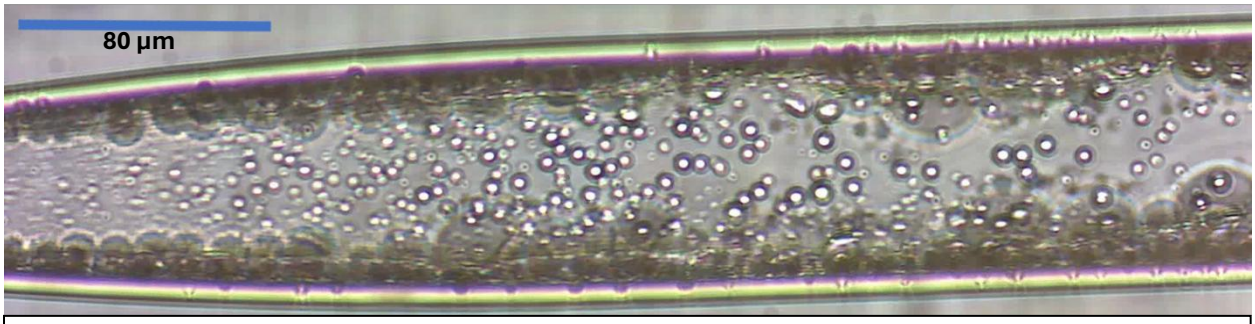

Figure 9: Visual of a control volume in an outlet channel carrying stabilized microdroplets with effective Glenium concentration at 8 mM. All the channels at the junction were 20 µm in width and the outlet is expanding to 80 µm gradually which is shown here.

On the other hand, the addition of Glenium caused another major obstruction in the form of foaming. Higher effective Glenium concentrations in outlets showed excessive foaming in the outlet channels, and droplets could not be observed due to thick foam clouds in between the camera and droplets. Therefore, an effective Glenium concentration of 8 mM in the outlet was determined to work best for getting satisfactory optical visuals. Although droplets were still colliding under relatively high flow speed, minimal coalescence of stabilized droplets was observed visually, as expected. Overall, these preliminary tests suggest that high-throughput microfluidic formation of stabilized droplets using Glenium is possible.

5 Conclusion

In summary, this study establishes a comprehensive experimental phase boundary for PDADMAC-PAA polyelectrolyte complex (PEC) dispersions through an in-depth investigation of composition. Consistent with the Voorn-Overbeek (V-O) model, the composition of supernatant and coacervate phases converges to unity as the initial polyelectrolyte concentration ($\Phi_{PE,0}$) increases, a phenomenon confirmed by experimental data and supported by rheological measurements. High-throughput turbidimetry further revealed an expanded phase boundary due to the influence of Glenium, highlighting its role in coacervate stabilization. The interplay between coacervate phase volume and polyelectrolyte concentration was found to govern the size and stability of PEC microdroplets, offering a pathway to tailor droplet characteristics for specific applications. The introduction of a microfluidic approach for monodisperse droplet generation marks a transformative advancement, overcoming limitations of traditional PEC systems. This approach enables precise control of droplet formation by modulating key parameters such as hydrostatic pressure and Capillary number, which can be fine-tuned through coacervate formulation and shear viscosity trends in this study instead of relying on device geometry. Collectively, this work provides a critical foundation for the rational design and engineering of PEC microdroplets, opening new possibilities for applications that require precise control of droplet size, stability, and functionality.

Thereafter, the direction of future work should focus on implementing this composition analysis to tailor protocell microreactors and evaluating the influence of PEC composition on the rate enhancement of reaction kinetics in stabilized microdroplets for cascade reactions. Simultaneously, a comprehensive investigation of microdroplet size variation should be conducted using dynamic light scattering analysis. This study should explore the effects of varying both cPE

and PE concentrations, expanding upon the current dataset, which only examines the influence of cPE on size distribution at a constant PE concentration of 70 mM. This set of experiments would help understanding the stabilization mechanism in-depth.

6 References

(1) OVERBEEK, J. T.; VOORN, M. J. Phase Separation in Polyelectrolyte Solutions; Theory of Complex Coacervation. *J Cell Physiol Suppl* **1957**, *49* (Suppl 1). https://doi.org/10.1002/jcp.1030490404.

(2) Srivastava, S.; Tirrell, M. V. Polyelectrolyte Complexation. In *Advances in Chemical Physics*; wiley, 2016; Vol. 161, pp 499–544. https://doi.org/10.1002/9781119290971.ch7.

(3) Dzieciol, A. J.; Mann, S. Designs for Life: Protocell Models in the Laboratory. *Chem Soc Rev* **2012**, *41* (1), 79–85. https://doi.org/10.1039/c1cs15211d.

(4) Mann, S. Systems of Creation: The Emergence of Life from Nonliving Matter. *Acc Chem Res* **2012**, *45* (12), 2131–2141. https://doi.org/10.1021/ar200281t.

(5) Holkar, A.; Gao, S.; Villaseñor, K.; Lake, M.; Srivastava, S. Quantitative Turbidimetric Characterization of Stabilized Complex Coacervate Dispersions. *Soft Matter* **2024**, *20* (26), 5060–5070. https://doi.org/10.1039/d3sm01761c.

(6) Li, L.; Srivastava, S.; Andreev, M.; Marciel, A. B.; De Pablo, J. J.; Tirrell, M. V. Phase Behavior and Salt Partitioning in Polyelectrolyte Complex Coacervates. *Macromolecules* **2018**, *51* (8), 2988–2995. https://doi.org/10.1021/acs.macromol.8b00238.

(7) van Swaay, D.; Tang, T. -Y. D.; Mann, S.; de Mello, A. Microfluidic Formation of Membrane-Free Aqueous Coacervate Droplets in Water. *Angewandte Chemie* **2015**, *127* (29), 8518–8521. https://doi.org/10.1002/ange.201502886.

(8) Gao, S.; Holkar, A.; Srivastava, S. Protein-Polyelectrolyte Complexes and Micellar Assemblies. *Polymers*. MDPI AG 2019. https://doi.org/10.3390/polym11071097.

(9) van den Berg, B.; Wain, R.; Dobson, C. M.; Ellis, R. J. Macromolecular Crowding Perturbs Protein Refolding Kinetics: Implications for Folding inside the Cell. *EMBO J* **2000**, *19* (15), 3870–3875. https://doi.org/10.1093/emboj/19.15.3870.

(10) Gao, S.; Holkar, A.; Srivastava, S. Protein-Polyelectrolyte Complexes and Micellar Assemblies. *Polymers*. MDPI AG 2019. https://doi.org/10.3390/polym11071097.

(11) Minton, A. P. Influence of Macromolecular Crowding upon the Stability and State of Association of Proteins: Predictions and Observations. *J Pharm Sci* **2005**, *94* (8), 1668–1675. https://doi.org/10.1002/jps.20417.

(12) Toor, R.; Hourdin, L.; Shanmugathasan, S.; Lefrançois, P.; Arbault, S.; Lapeyre, V.; Bouffier, L.; Douliez, J. P.; Ravaine, V.; Perro, A. Enzymatic Cascade Reaction in Simple-Coacervates. *J Colloid Interface Sci* **2023**, *629*, 46–54. https://doi.org/10.1016/j.jcis.2022.09.019.

(13) Karlsson, M.; Davidson, M.; Karlsson, R.; Karlsson, A.; Bergenholtz, J.; Konkoli, Z.; Jesorka, A.; Lobovkina, T.; Hurtig, J.; Voinova, M.; Orwar, O. Biomimetic Nanoscale Reactors and Networks. *Annual Review of Physical Chemistry*. Annual Reviews Inc. 2004, pp 613–649. https://doi.org/10.1146/annurev.physchem.55.091602.094319.

(14) Bezrukov, A.; Galyametdinov, Y. Tuning Properties of Polyelectrolyte-Surfactant Associates in Two-Phase Microfluidic Flows. *Polymers (Basel)* **2022**, *14* (24). https://doi.org/10.3390/polym14245480.

(15) Gao, S.; Srivastava, S. Comb Polyelectrolytes Stabilize Complex Coacervate Microdroplet Dispersions. *ACS Macro Lett* **2022**, *11* (7), 902–909. https://doi.org/10.1021/acsmacrolett.2c00327.

(16) Huebner, A.; Sharma, S.; Srisa-Art, M.; Hollfelder, F.; Edel, J. B.; DeMello, A. J. Microdroplets: A Sea of Applications? *Lab on a Chip*. Royal Society of Chemistry 2008, pp 1244–1254. https://doi.org/10.1039/b806405a.

(17) Teh, S. Y.; Lin, R.; Hung, L. H.; Lee, A. P. Droplet Microfluidics. *Lab on a Chip*. Royal Society of Chemistry 2008, pp 198–220. https://doi.org/10.1039/b715524g.

(18) Ibrahim, A. M.; Padovani, J. I.; Howe, R. T.; Anis, Y. H. Modeling of Droplet Generation in a Microfluidic Flow-Focusing Junction for Droplet Size Control. *Micromachines (Basel)* **2021**, *12* (6). https://doi.org/10.3390/mi12060590.

(19) Dittrich, P. S.; Jahnz, M.; Schwille, P. A New Embedded Process for Compartmentalized Cell-Free Protein Expression and on-Line Detection in Microfluidic Devices. *ChemBioChem* **2005**, *6* (5), 811–814. https://doi.org/10.1002/cbic.200400321.

(20) Moon, B. U.; Abbasi, N.; Jones, S. G.; Hwang, D. K.; Tsai, S. S. H. Water-in-Water Droplets by Passive Microfluidic Flow Focusing. *Anal Chem* **2016**, *88* (7), 3982–3989. https://doi.org/10.1021/acs.analchem.6b00225.

(21) Fallah-Araghi, A.; Baret, J. C.; Ryckelynck, M.; Griffiths, A. D. A Completely in Vitro Ultrahigh-Throughput Droplet-Based Microfluidic Screening System for Protein Engineering and Directed Evolution. *Lab Chip* **2012**, *12* (5), 882–891. https://doi.org/10.1039/c2lc21035e.